Automotive and Engine Technology (2025) 10:4
https://doi.org/10.1007/s41104-025-00151-z

ORIGINAL PAPER

Simultaneous LIF and BOS investigation of an impact of a gaseous jet on an oil film under engine relevant conditions

J. Reimer[1] · M. Maliha[1] · H. Kubach[1] · T. Koch[1]

Received: 28 January 2025 / Accepted: 7 April 2025

Abstract
Internal combustion engines are a significant contributor to global CO_2 emissions. Sustainable fuels are seen as having great potential to significantly reduce these emissions. Hydrogen has the potential to significantly reduce local emissions. It can also be injected directly into the combustion chamber, where the resulting jet interacts with the cylinder wall and can influence the engine process. To be able to quantify this influence, fuel impingement has been investigated in this work. As fluids with different states of aggregation interact with each other in this process, a special measurement technique has to be applied. The gaseous fuel is visualised using a background oriented schlieren technique. The liquid phase of the oil is visualised using laser induced fluorescence. Using this technique, it was observed that the impact of a gaseous jet can deform a thin oil film and that isolated detachment effects can be observed.

Keywords LIF · BOS · LIF-BOS-combination · Interaction

List of Symbols

BOS	Background oriented schlieren
CCD	Charge-coupled device
CO_2	Carbon dioxide
DI	Direct injection
f	Focal length
LED	Light-emitting diode
LIF	laser-induced fluorescence
OH	Hydroxyl radical
u	Atomic unit of measurement for weight
UV	Ultra violet
Δy	Image shift
Z_A	Distance between the lens and the measurement area
Z_D	Distance between the background pattern and the density gradient
σ	Surface tension of the fuel
Φ	Impact angle
ε_y	Deflection angle

1 Introduction

Internal combustion engines contribute significantly to global CO_2 emissions. It is one of the biggest challenges to reduce these emissions. One way is to use hydrogen as a fuel [1]. However, the use of hydrogen has a major influence on the engine process, which is why this is the focus of many research projects. The location of mixture formation, whether inside or outside the combustion chamber, has different potentials but also challenges, which is widely discussed in the literature. However, if the fuel is introduced directly into the combustion chamber, interactions can occur between the hydrogen and the oil wetted cylinder wall. These processes have already been studied and discussed several times for the use of liquid fuels, but are also not yet fully understood. The interaction processes can have an influence on the emission behaviour, but also on combustion anomalies, such as pre-ignition. Especially the pre-ignition behaviour is a crucial and not yet understood phenomenon in engine gasoline and hydrogen combustion, which still limits the full development of the potential in terms of performance and durability. For this reason, it is important to research these processes and thus contribute to the understanding of the system.

To be able to observe this phenomenon simultaneously in the experiment, it must be possible to observe the gas and liquid phases separately. For this purpose, two colours can

✉ J. Reimer
jan.reimer@kit.edu

[1] Institute of Internal Combustion Engines (IFKM), Karlsruhe Institute of Technology, Rintheimer Querallee 2, Building 70.03, 76131 Karlsruhe, Germany

Published online: 21 April 2025

be used for the exposure, which are later separated from each other by a filter and the different information is recorded by two cameras. One way to study this phenomenon is to mix the liquid phase of the oil with tracers and excite it, using the laser-induced fluorescence-principle. The gas jet can be visualised using the Background Oriented Schlieren method. In this study, the focus is on the design and application of the measurement setup. In addition, a suitable method is presented that visualises the results. Finally, selected results are presented to address the phenomenological question of how an impact of a gas jet can influence an oil film.

2 State of knowledge

2.1 Interaction between spray/jet and oil film

Various phenomena can be observed when liquid droplets impinge on a liquid film. The initially stationary film is deformed by the impact, which is mainly influenced by the momentum of the incident spray and the properties of the oil film. As a result, characteristic waves are formed [2, 3]. These become larger as the energy state of the incident fluid increases, until the crown becomes unstable due to its own inertia and droplets can detach from it, which are known as splashing droplets. This phenomenon is characterised by the fact that the droplets are smaller than those of the primary spray and are formed shortly after the impact. Dimensionless parameters (Reynolds-Weber number or K-factor) are used to describe the physical processes as accurately as possible when liquid droplets impact [4–6]. It is also known that secondary droplets can form due to the shear force of the spray-induced flow at the crests of the waves. These droplets can be larger than the initial oil film thickness and are formed with a time delay to the splashing droplets. The formation mechanisms are mainly dependent on the flow velocity induced at the film surface and the deformation and physical properties of the oil film [7, 8]. In addition, fluid deposits on and air inclusions in the oil film can be observed during spray impingement. These mechanisms are not so well described in the literature for the impact of gaseous jets. This work should therefore contribute to a better understanding of the processes involved in the impact of gaseous jets.

2.2 Laser-induced fluorescence (LIF)

Laser-induced fluorescence (LIF) is a widely used technique for the high-resolution analysis of complex processes. It is based on the phenomenon that certain substances can be excited by a light source. After a very small time delay, the absorbed light can be emitted with a red shift, the so-called Stokes shift. The LIF principle and the most important influencing parameters are well described in the literature [9–12]. The spectral shift allows the LIF fluorescence to be spectrally separated from the excitation source. This makes it possible to observe and detect even low concentrations of the target liquid, such as thin films of liquid inside the engine. [13] observed thin oil films on the cylinder wall. [12] used the LIF technique to determine oil film thickness during engine operation. Fuel films that may form inside the engine can also be studied using this measurement technique [14]. The LIF technique is also used to visualise the OH-rich flame front of stoichiometric oxidation [15, 16].

In this work, a light emitting diode (LED) was used to optically excite liquid components. An Inolux IN-C68QA(X) TM UV with a power of 10 W and a peak wavelength of 365 nm was used. To increase the excitation intensity and thus also the image quality, four of these LEDs were connected in series. The quality of the commercial LED was investigated using a spectrograph. A 150 lines/mm optical grating was used for spectral distribution and a PI-MAX 2 camera for optical recording. A detailed description of the instrument and the measurement technique is given in [17]. The resulting spectrum, normalised to the maximum value, is shown in Fig. 1 (purple curve). It can be seen that the

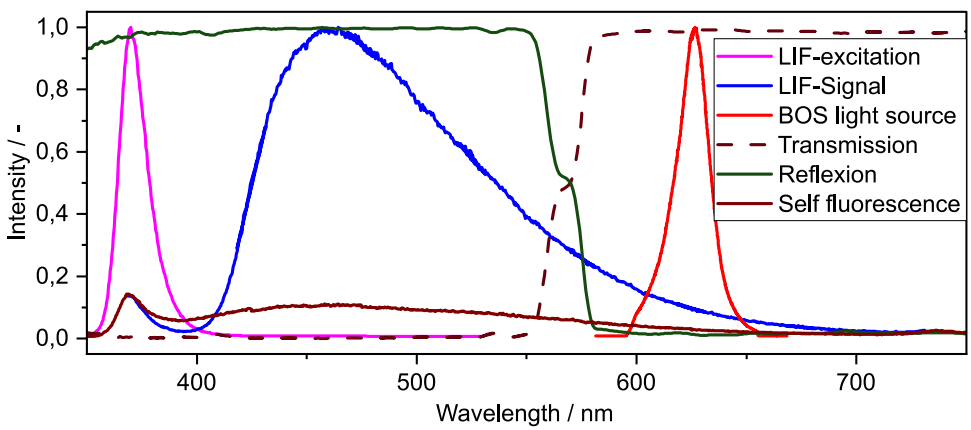

Fig. 1 Relevant spectral data: LIF- and BOS-colour channel and behaviour of the dichroic filter

position of the peak wavelength agrees well with the data sheet. It should also be noted that there is no significant excitation at wavelengths above 400 nm.

The used oil is Total Quartz 700 EGY10 W40(SN) engine oil. Since oils with additives can have a non-negligible intrinsic fluorescence, especially compared to short wavelength excitation light sources, the detected intrinsic fluorescence is shown in Fig. 1 (brown curve). It can be seen that the intensity is low, so a fluorescence tracer must be used to improve the measurement quality. Tracers are substances with particularly good absorption and emission properties. If they are sufficiently soluble, they can be added to the liquid under investigation. In this work, a tracer from Honeywell called LumiluxBlue was used. It has good solubility in engine oils [8] and good absorption behaviour in the UV range. Figure 1 (blue curve) shows a LIF-Signal normalised to the intensity maximum for the used tracer concentration of 1000 mg/l in the oil used. This tracer concentration led to a completely saturated oil and no further increase in concentration was possible. The fluorescence signal shows that the intensity maximum is around 460 nm, which provides good spectral separation from the excitation source.

2.3 Background oriented schlieren (BOS)

The Background Oriented Schlieren method allows to analyse colourless gas with a simple construction. The prerequisite for this is that the gas to be analysed has a different density than the environment. In contrast to the conventional schlieren method, no long paths and large parabolic mirrors are required, but only a point pattern and a camera. This technique was introduced by Dalziel [18] (1998) and Meier [19] (1997) and is schematically shown in Fig. 2.

The illumination of the background pattern for the application of the BOS technique was realised with a red LED. The diode with the designation OSRAM OSRAM OSTAR Projection Power, LE A P3MQ was used. This is a high-power diode with a maximum power consumption of 110 W. The spectral characteristics are shown in Fig. 1 (red curve). The relevant intensities of this diode are between approx. 590 and 660 nm, with the intensity maximum at approx. 625 nm.

For measurement, a reference image of the background without analysis gas is generated in the measuring area. Then each image of the experiment is compared with the reference image. The images can be evaluated by an image correlation method. Evaluation algorithms, such as those used in particle image velocimetry, can then evaluate the displacement of the pattern at different locations in the image [20].

The experimental setup is explained in chapter 3.2.

Taking a paraxial image with small deflection angles ($\varepsilon_y \approx \tan \varepsilon_y$) the image shift, according to Raffel [20], can be described as follows

$$\Delta y = f\left(\frac{Z_D}{Z_D + Z_A - f}\right)\varepsilon_y \tag{1}$$

Here, Z_D is the distance between the background pattern and the density gradient, Z_A is the distance between the lens and the measurement area, ε_y is the deflection angle, and f is the focal length of the lens. If the lens is focussed on the background, the following applies

$$\frac{1}{f} = \frac{1}{Z_i} + \frac{1}{Z_B} \tag{2}$$

Equation (1) shows that large image shifts can only be achieved if Z_D is large and Z_A is small. The maximum image shift with increasing Z_D can be described approximately

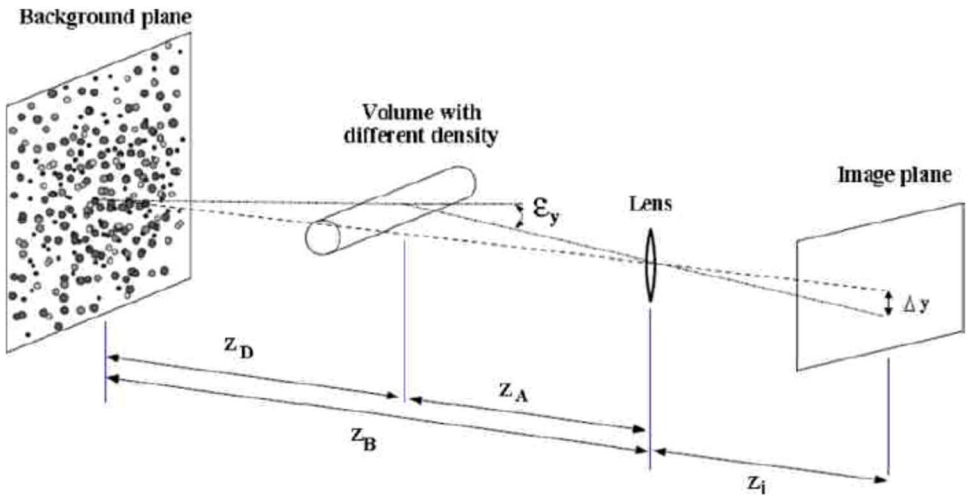

Fig. 2 BOS imaging configuration [20]

Table 1 relevant properties of hydrogen and helium for a quantitative comparison

	Helium	Hydrogen
Ignition temperature	Not inflammable	600 °C
Density	0.1785 kg/m^3	0.08988 kg/m^3
Molar mass	Ca. 4 u	Ca. 2 u
Boiling temperature	− 268,9 °C	− 252,9 °C

with $\Delta y = f\varepsilon_y$. However, as Z_A decreases, certain boundary conditions must be observed to keep the flow field sufficiently sharp. Since the system is focussed on the background, the sharpness of the examined density gradient decreases with decreasing Z_A [20]. One approach to solving this is to use the largest possible f-number of the lens used to maximise the depth of field.

3 Experimental setup

3.1 Gaseous jet

This chapter describes the boundary conditions that are necessary to generate the gaseous fuel jet. Table 1 lists relevant properties of the fluids used. Since hydrogen is a highly flammable substance, strict and elaborate safety precautions must be ensured for real use. These can significantly increase the complexity of the periphery of the experimental setup. To limit this additional expense, helium was used as an inert surrogate in this study, since it makes little or no difference to the beam propagation [21].

The comparability of these two substances has been methodically analysed and described in the literature [15]. It has been shown that the volume of gas produced is very similar for both substances. With this assumption, helium, which has twice the density of hydrogen, produces twice the mass hitting the oil film. The gas also has a higher inertia. As these material properties mean that the effect of the impact must be more critical and more pronounced with helium than with hydrogen, a more critical case is considered in the experiments. If there is no change in the oil film due to the impact of helium, then no change is to be expected with hydrogen. Otherwise, the tests should be repeated with hydrogen.

Different injection strategies are being pursued in the development of hydrogen engines. Basically, one can distinguish between three strategies: intake manifold injection, low-pressure injection and high-pressure injection. Since only hydrogen injected directly into the combustion chamber is expected to interact significantly with the oil-wetted cylinder wall, possible injectors for the intake tract were not considered. The formation and shape of the hydrogen jet can significantly influence the mixture formation and thus also the emission behaviour of the engine. For this reason, so-called injector caps are being investigated and used. These can significantly influence the shape of the jet and can consequently also influence the impact behaviour on the cylinder wall. To limit the number of parameters for the test, the use of possible caps was dispensed with. An injector that can be used as a DI injector for gaseous fuels at high pressures is the Bosch HDEV4. This is a piezo-actuated injector with a mechanical load limit of 200 bar. The needle is an outward-opening A-nozzle, which results in a jet shape that is similar to the letter A.

The injector is controlled by a single injection control unit from the manufacturer ScienceLab. This control unit makes it possible to change the relevant injection parameters. In addition, a 300-bar helium compressed gas bottle was connected to the injector. An adjustable pressure reducer was fitted between these components to allow the fuel pressure to be varied. Table 2 shows all relevant injection parameters used in this study.

Figure 3 shows a series of images of the gaseous jet used, which was recorded using the BOS technique. Picture 1 shows the moment shortly before the start of injection, Picture 2 the moment shortly after the start of injection and Picture 3 the timing approx. 700 µs after the start of injection. It can be seen that at the beginning of the injection the typical jet shape for A-nozzles is formed. With increasing distance to the injector needle, however, the opening angle of the jet reduces and leads to an increasingly cylindrical shape of the jet. Using self-developed scripts of the tool Matlab, an indentation velocity could be calculated. Using functionalities such as edge detection, the location of the deepest penetrated hydrogen can be marked. With the help of the local and temporal resolution of the optical detection, which are shown in Table 3, the speed of travel of the jet front can be calculated from this. Only the part of the velocity that runs parallel to the injector axis was considered. As described many times in the literature, the impact velocity of the incident jet can influence the interaction process. For the jet used in this work, this results in an average penetration velocity of approx. 38 m/s. The average penetration

Table 2 relevant parameter for the injection

Parameter	Unit	Value
Injection duration	µs	5000
Injection pressure	bar	40
Impact angle	°	90
Impact distance	mm	50
Injected substance	–	Helium

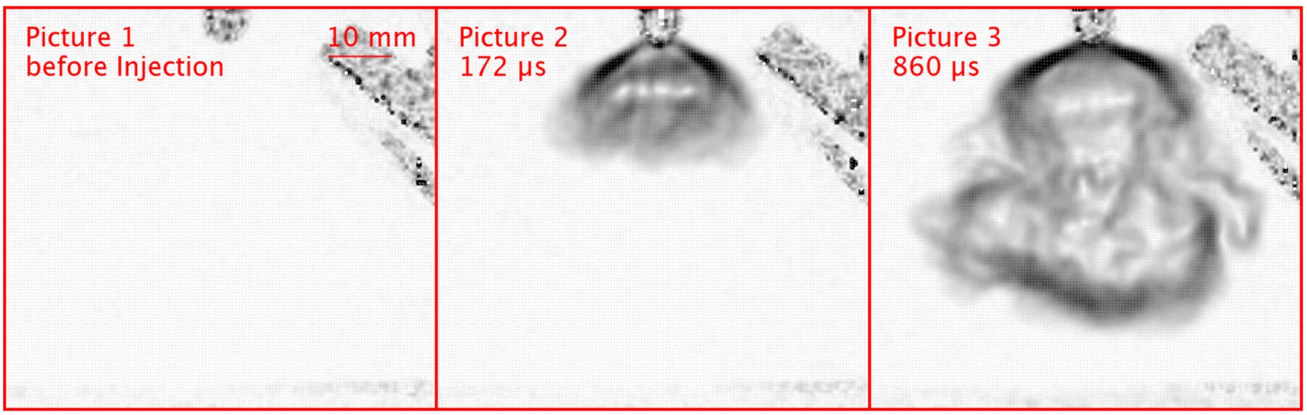

Fig. 3 Illustration of the gaseous jet, shortly before (Fig. 1), shortly after (Fig. 2) and 700 µs after the injection

Table 3 relevant properties of the camera setup

Sensor type	12-bit CMOS
Pixels	1024×1024
Pixel size	20 µm
Spatial resolution	54 µm/Pixel
Frame rate	5.8 kHz
Temporal resolution	Ca. 171 µs/Picture

velocity is the propagation velocity of the jet front between pictures 2 and 3 (Fig. 3).

3.2 Measurement setup

To evaluate the same jet recording with BOS and LIF, it is necessary to use two cameras. For this purpose, two high-speed cameras (Photron HSS6) were used. To use the measurement techniques independently, the oil is excited with a UV LED (365 nm/40 W) and for the BOS images a red LED (626 nm/110 W) is used. To pick up the superimposed light individually with the cameras, a dichroic filter is used to reflect the wavelength from 0 to 567 nm and transmit the remaining range. The spectral characteristics of the filter are shown in Fig. 1.

The two cameras also allowed different focal planes to be used. For the LIF images, this was aligned so that the detaching droplets were in the focal plane. For the BOS images, it is important that the background pattern is in focus.

The injector is aligned from above at a distance of 50 mm and an angle of 90° to the oil-wetted surface. The background pattern for the BOS calculation is in front of the red LED. This was printed on a transparent foil and covered with frosted glass foil. This creates a more homogeneous brightness distribution and therefore a better contrast between the dots and the background. The distance between the background pattern and the measurement volume Z_D is 60 mm and between the measurement volume and the

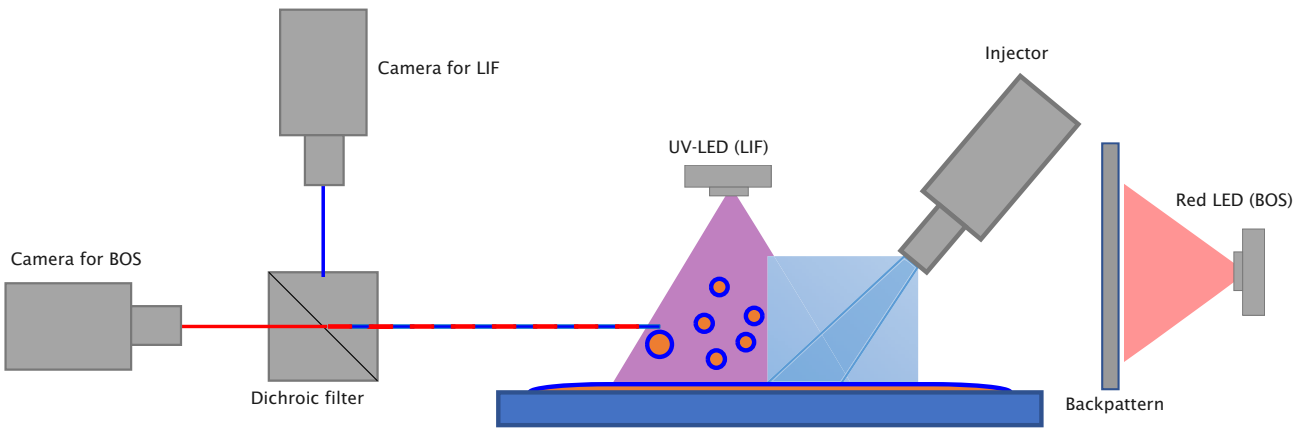

Fig. 4 Measurement setup for LIF and BOS

camera lens Z_A is 180 mm. To better understand the setup, it is shown schematically in Fig. 4.

The relevance of the selected geometric boundary conditions depends heavily on the specific application of the motor. For small engine classes, which are frequently found in the passenger car sector, a distance of 50 mm is realistic. The larger the engine displacement, the greater the distance between the injector and the impact plane should be. A range between 30 and 75° is more relevant for engine processes than the 90° case investigated here. As this work only focussed on the feasibility of this technology, it was not possible to carry out a detailed sensitivity analysis with regard to the impact angle. The used propagation velocity is therefore seen as representative for specific applications.

3.3 Methodology

The purpose of this chapter is to describe the methodology of how the data was handled. Today's camera sensors that capture the graphical data usually consist of light sensitive devices (charge-coupled device-CCD) that can convert the incident light intensity into an electrical signal. Today's camera chip consists of a string of these CCDs, whereby the electrical information of a CCD is converted as a pixel value and thus the image is built up. In the case of colour images, each pixel is divided into four CCDs, which have different sensitivities to the incident wavelength. For this purpose, the use of the so-called Bayer sensor has become widely accepted. This divides a pixel into two green, one red and one blue component. The structure of the digital image is usually subdivided in a simplified way into a green, blue and red segment each, a so-called RGB matrix. A mixed colour can then be graphically reproduced from the individual colour components. The individual components can have values between 0 and 255. This digital structure was used to display the information from the different cameras in one image.

First, the optical offset between the two cameras was compensated. This error is caused by the misalignment of the camera and the dichroic filter. To do this, an M6 screw was positioned in the observation space and captured simultaneously by both cameras. Both images were digitally transferred into one image, which is shown in Fig. 5. The combined image contains only information from the camera for BOS in its red components (see Fig. 4) and the information from the camera for LIF in its blue component. This allows an offset to be defined in the x (Fig. 5, yellow arrow) and y (Fig. 5, green arrow) directions, which must be considered when superimposing two images.

Figure 6 shows the analysis methodology schematically. The left image shows the raw image with jet taken by the BOS camera. Here, mainly the background pattern can be seen. The second image shows the result of the applied BOS

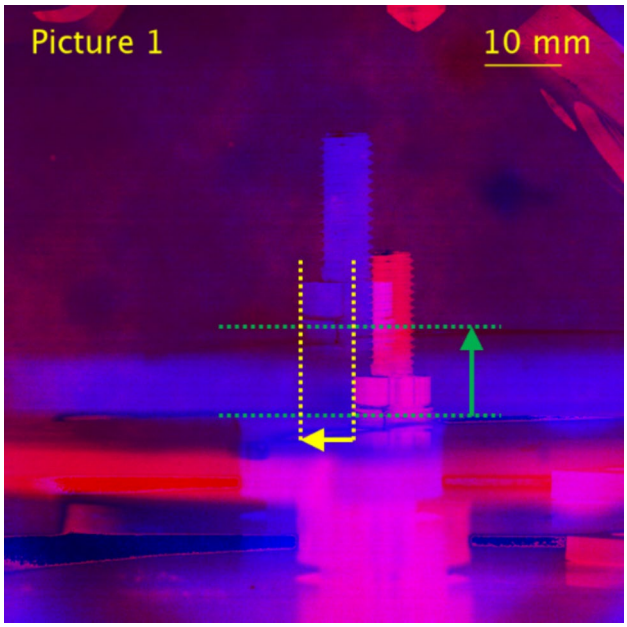

Fig. 5 Schematic figure of the offset between both cameras

algorithm as described in [21]. Yofu can see the jet, which is shown in greyscale. The third image shows the image information of the gas jet, converted into a colour image. The image information is only used as the red part of the colour image. After taking the graphic offset into account, the LIF information can be superimposed in the last calculation step. These are only transferred to the blue channel of the colour image. The result is the right-hand image of Fig. 6, which contains the location and time-simultaneous information of the LIF and BOS technology.

4 Results

In the following, the experimental results are presented and the observations are discussed and analysed. For this purpose, two tests were carried out with the same jet parameters (see table 2), but with different properties of the oil film. First, the interaction with a thick, cold oil film was investigated. Therefore, an oil amount of 5 ml was applied to the sample plate and an arbitrary distribution of the oil over the surface was arranged. The resulting oil film thickness is not reproducible to adjust, but this method allows high-quality images to be obtained as a distinct LIF signal can be achieved. It is expected that the part effects can be perceived more strongly during the interaction. To investigate the effects under engine-like conditions, an interaction with a heated and thin oil film was also investigated. For this purpose, the oil film with a thickness of 80 µm was

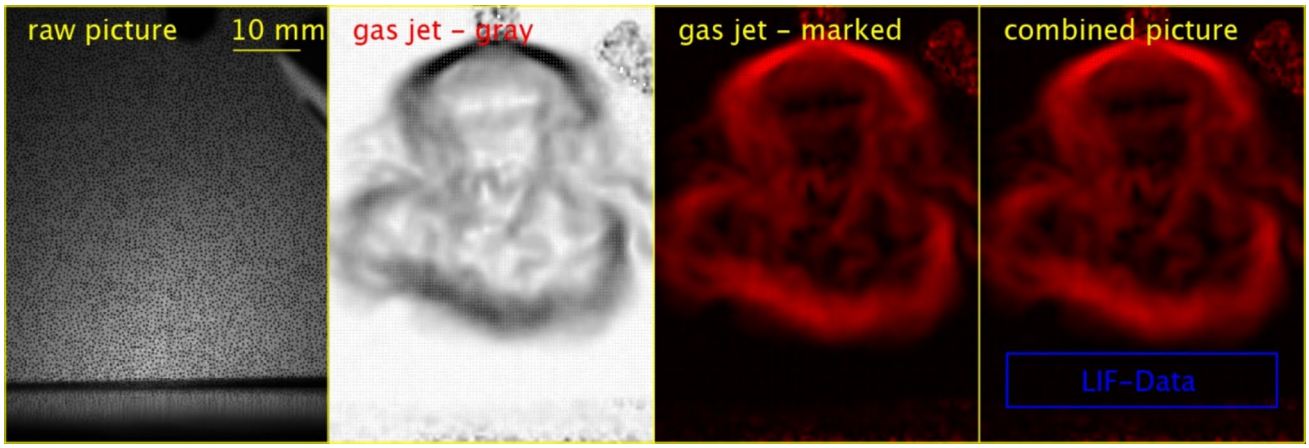

Fig. 6 Methodology of post-processing to show the LIF and BOS techniques simultaneously

produced. This was achieved with the help of the rotational movement of a spin coater, which is described in [8]. In addition, a heating wire integrated into the sample plate was used to heat the sample plate and thus also the oil to a temperature of 90 °C.

4.1 Impact on a cold, thick oil film

The impact behaviour of a gaseous jet is presented as a series of pictures in Fig. 7. The gaseous phase of the jet is shown in red and the liquid phase of the oil in blue. The time of impact is shown in the second picture. In the fourth image, the first recognisable change in the oil film can be seen, which is approx. 1700 µs after the start of the interaction. In the further course, a clear deformation of the oil film can be observed. To illustrate the processes that the oil film undergoes, a selected point in time is shown enlarged in Fig. 8. With the information of the local resolution of the image, the maximum deformation of the oil film was determined to be approx. 900 µm. In addition, isolated detachment effects can be seen on the oil film surface. This effect is described several times in the literature [7, 22]. In this case, the gas flow on the surface of the liquid applies a shearing force that can detach individual ligaments from the liquid film when the surface tension is overcome. Compared to the impact behaviour of a spray, which consists of liquid droplets, it can be summarised that known splashing effects cannot be detected. This is mainly explained by the fact that the density of the incident fluid is significantly lower for

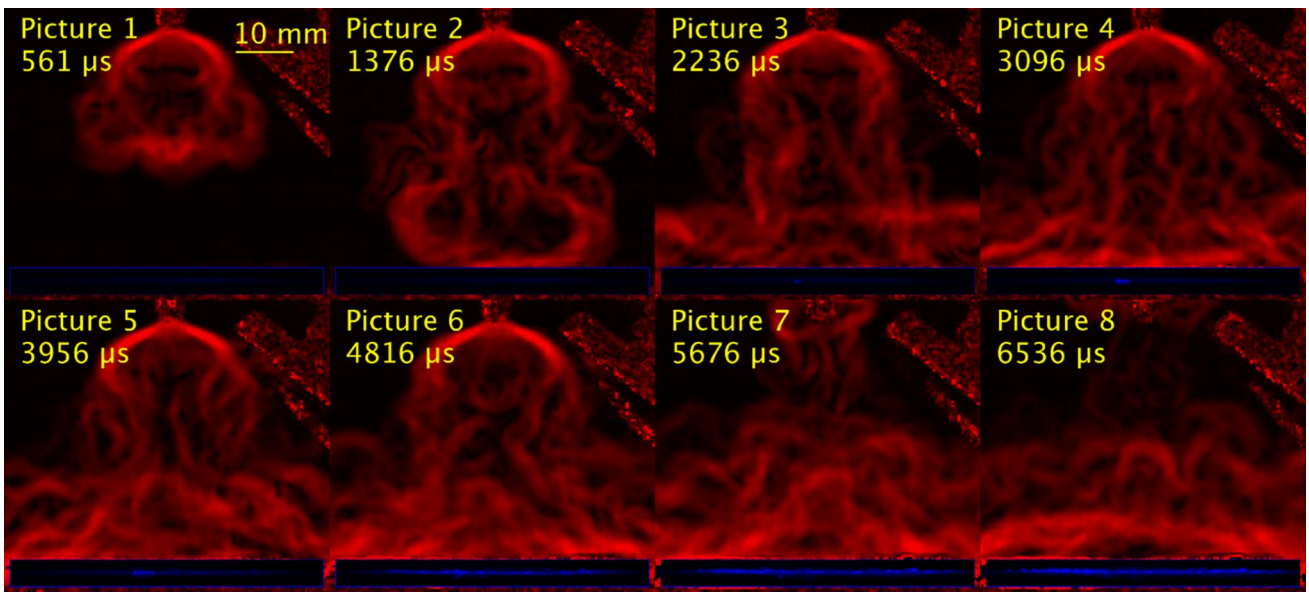

Fig. 7 Picture series of an impingement of a gaseous jet (red coloured) on an cold oil film (blue coloured)

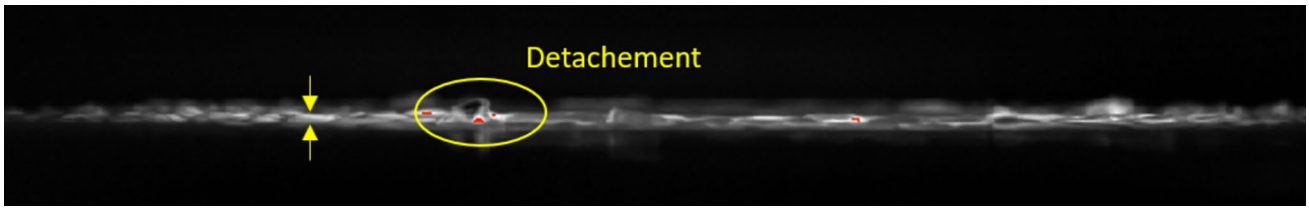

Fig. 8 Deformation of the oil film due to an impingement of a gas jet

the gas phase. In addition, the large time offset between the onset of impact and the first observable oil film deformation should be mentioned. But the effects of oil film deformation and detachment of ligaments, which are shown in Fig. 8, can be observed for the gaseous jet and the liquid fuel spray impingement [8, 23, 24].

4.2 Impact on a hot, thin oil film

As described earlier, Fig. 9 shows the graphical data of the impact of a gas jet on a thin heated oil film. The images have been simplified and only show the enlarged LIF portion of the liquid phase to illustrate the effects. This made it possible to increase the frame rate to 10 kHz, which improved the temporal resolution. It can be seen that the temporal offset between the impact and the first observable oil film deformation is reduced to about 1000 µs. This can be explained mainly by the lower viscosity of the oil at a temperature of 90 °C. This property is to be understood as a measure of resistance to deformation, which decreases with increasing temperature and thus simplifies deformation. Furthermore, the deformation of the oil film could be determined to a maximum oil film height of approx. 750 µm with the help of the local resolution of the image. And local detachment effects can also be seen in Fig. 9 in Picture 4 and 5. This can be explained mainly by the reduced surface tension as a result of the temperature increase. This seems to overcompensate for the reduced impact surface resulting from a lower oil film deformation compared to the cold oil.

The size of the detached ligaments observed here can be bigger than 100 µm and the speed of movement approx. 15 m/s. These values were determined using local and temporal resolution of the images. The magnitude of these properties is similar to interaction processes of liquid fuel spray with an oil film [7, 8], which is taken as an indication that comparable formation mechanisms are involved.

4.3 Comparing the impact of a spray and a jet on an oil film

As described in [8], the impact of a liquid spray can be divided into various sub-phenomena. Figure 9 from [8] shows an example of this. The formation of splashing droplets (fog), which can be seen in picture 2 in Fig. 10, cannot be observed during the impact of a jet. The main reason for this is that the impact area is much larger when a gaseous jet is impacted. Whilst individual droplets hit a very small oil surface in a spray, the front of the jet hits the oil film as a whole. Therefore, there are no comparable dimensionless indicators that can be used to predict splashing (K-factor [5]). The deformation of the oil film by observing waves on the oil film can be recognised for both the impact of the spray and the jet. As a result of this deformation, the detachment of large, shear-induced secondary droplets is observed on the impact of a gaseous jet. However, the number of these droplets is significantly lower compared to the spray. As the propagation speed of the jet and the spray used here for both is 30–40 m/s and the properties of the oil film are of a similar order of magnitude, it is concluded that the deformation of the oil film must be significantly greater in the case of the spray. The other phenomena, foaming and fluid accumulation on the oil film surface, cannot be observed for the impact of a

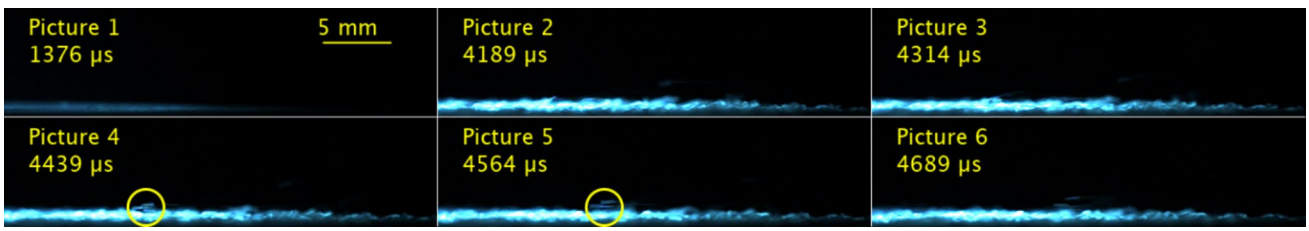

Fig. 9 Picture series of a gas jet impingement on a hot oil film

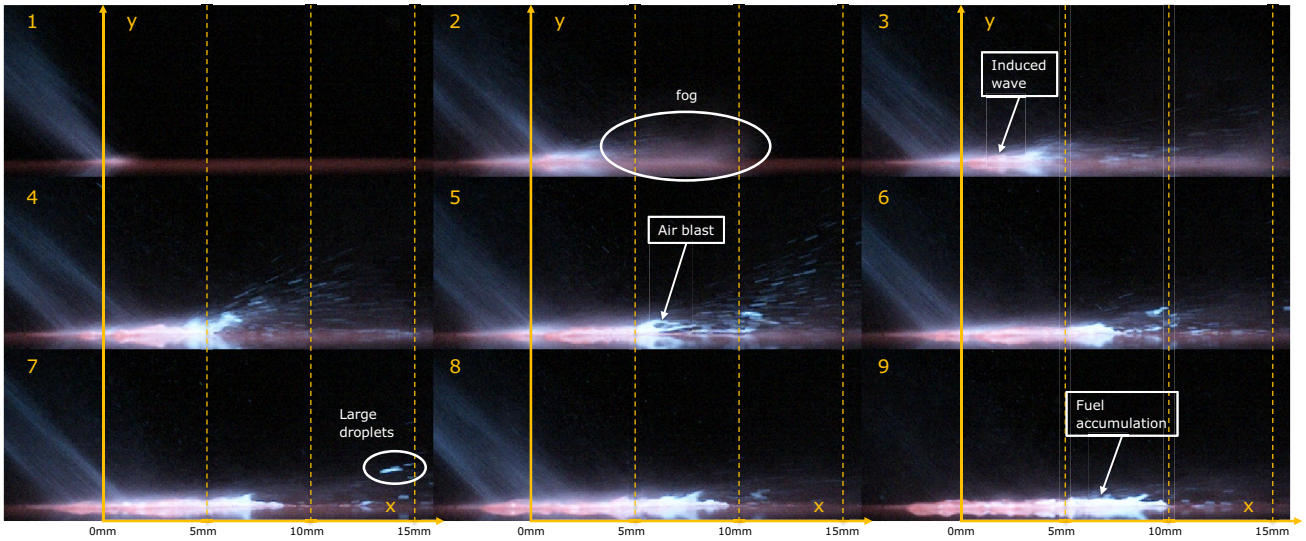

Fig. 10 Overview of the characteristic partial phenomena on impact of a liquid spray on an oil film [8]

gaseous spray. The absence of foaming is explained by the fact that the impact of a jet is a full-surface interaction. The impact area is much larger and therefore the local maximum impulse must be smaller for a jet than for a spray.

5 Summary and conclusions

In this work, a methodology is applied for the simultaneous, optical detection of interaction processes between fluids of different aggregate states. An impact event between a gaseous jet and an oil film lying on a rigid wall should be investigated. For this purpose, a BOS technique was applied to graphically represent a gaseous fluid. The liquid phase of the investigated processes was visualised with a qualitative LIF technique. The experimental setup used and described in this work is well suited for this application. The key factor is the use of two cameras, as different focal planes are required for the different imaging techniques. The spectral separation was realised using different wavelength ranges of the imaging techniques. The appropriate light information was directed to the target camera using a dichroic filter. Finally, suitable post-processing is necessary, which overlays the images from the individual cameras. For this purpose, the image information was marked with false colours and displayed simultaneously but optically separable in a combined image. This made it possible to observe and analyse the interaction processes that take place when a gaseous jet hits an oil film.

With this methodology, the impact effects could be observed and analysed. Results indicate that an impact of a gas jet can significantly influence and change an oil film. In addition to the deformation of the initially uniform film, isolated detachment effects and the formation of secondary droplets could also be observed. The formation mechanism of secondary drops, which is based on splashing and is known from the impact of liquid fuel on an oil film, could not be observed in this study. However, the determination of the exact boundary conditions for these individual effects must be specifically investigated separately in extensive parameter and sensitivity studies. For engine applications, however, it can be concluded that the impact of a gas jet on the cylinder wall influences the combustion and emission behaviour and therefore cannot be neglected.

Acknowledgements This work was supported by the Deutsche Forschungsgemeinschaft (DFG – German Research Foundation) Project number 237267381 Collaborative Research Center/Transregio 150 'Turbulent, chemically reactive, multi-phase flows near walls'. The authors want to thank the DFG for funding this project.

Author contributions JR and MM wrote the manuscript text and all authors reviewed the manuscript.

Funding Open Access funding enabled and organized by Projekt DEAL.

Data availability No datasets were generated or analysed during the current study.

Declarations

Competing interest The authors declare no competing interests.

References

1. Lott, P., Wagner, U., Koch, T., Deutschmann, O.: "Der Wasserstoffmotor – Chancen und Herausforderungen auf dem Weg zu einer dekarbonisierten Mobilität," (in german). Chemie Ingenieur Technik **94**(3), 217–229 (2022). https://doi.org/10.1002/cite.202100155
2. Liang, G., Mudawar, I.: Review of mass and momentum interactions during drop impact on a liquid film. Int. J. Heat Mass Transfer **101**, 577–599 (2016). https://doi.org/10.1016/j.ijheatmasstransfer.2016.05.062
3. Liang, G., Guo, Y., Shen, S., Yu, H.: A study of a single liquid drop impact on inclined wetted surfaces. Acta Mech. **225**(12), 3353–3363 (2014). https://doi.org/10.1007/s00707-014-1110-8
4. Stumpf, B., Ruesch, J., Roisman, I.V., Tropea, C., Hussong, J.: An imaging technique for determining the volume fraction of two-component droplets of immiscible fluids. Exp Fluids (2022). https://doi.org/10.1007/s00348-022-03462-1
5. Kittel, H., Roisman, I.V., Tropea, C.: Splash of a drop impacting onto a solid substrate wetted by a thin film of another liquid. Phys. Rev. Fluids (2018). https://doi.org/10.1103/PhysRevFluids.3.073601
6. Xu, L., Barcos, L., Nagel, S.R.: "Splashing of liquids: interplay of surface roughness with surrounding gas." Phys. Rev. Stat. Nonlinear Soft Matter Phys. **76**(6 Pt 2), 66311 (2007). https://doi.org/10.1103/PhysRevE.76.066311
7. Opfer, L., Roisman, I.V., Tropea, C.: Primary Atomization in an Airblast Gas Turbine Atomizer. Springer, Dordrecht (2013)
8. Maliha, M., et al.: Optical investigation on the interaction between a fuel-spray and an oil wetted wall with the focus on secondary droplets. Int. J. Eng. Res. **24**(4), 1578–1588 (2023). https://doi.org/10.1177/14680874221095235
9. Rüttinger, S., Spille, C., Hoffmann, M., Schlüter, M.: Laser-induced fluorescence in multiphase systems. ChemBioEng. Rev. **5**(4), 253–269 (2018). https://doi.org/10.1002/cben.201800005
10. Weimar, H.-J.: Entwicklung eines laser-optischen Messystems zur kurbelwinkelaufgelösten Bestimmung der Ölfilmdicke zwischen Kolbenring und Zylinderwand in einem Ottomotor, 5th edn. Logos Verlag Berlin, Berlin (2022)
11. Wiggers, S.: Charakterisierung von Öl- und Kraftstoffschichten in der Kolbengruppe mittels laserinduzierter Fluoreszenz. Duisburg-Essen, (2014). https://core.ac.uk/download/pdf/33797291.pdfhttps://core.ac.uk/download/pdf/33797291.pdf
12. Müller, T.: "Simultane Visualisierung von Öl- und Kraftstoffschichten in der Kolbengruppe eines direkteinspritzenden Ottomotors durch laserinduzierte Fluoreszenz. Duisburg, Essen (2018)
13. Schweizer, T., Kubach, H., Koch, T.: Investigations to characterize the interactions of light radiation, engine operating media and fluorescence tracers for the use of qualitative light-induced fluorescence in engine systems. Automot. Eng. Technol. **6**(3–4), 275–287 (2021). https://doi.org/10.1007/s41104-021-00092-3
14. Kambe, H., Mizobuchi, N., Matsumura, E.: "simultaneous measurement of fuel droplet deposition amount and oil film thickness on spray impingement using double laser induced fluorescence method." In: SAE Technical Paper Series, (2017)
15. Li, T., Schiemann, M., Köser, J., Dreizler, A., Böhm, B.: Experimental investigations of single particle and particle group combustion in a laminar flow reactor using simultaneous volumetric OH-LIF imaging and diffuse backlight-illumination. Renew. Sustain. Energy Rev. **136**, 110377 (2021). https://doi.org/10.1016/j.rser.2020.110377
16. Ma, X., Xu, H., Jiang, C., Shuai, S.: Ultra-high speed imaging and OH-LIF study of DMF and MF combustion in a DISI optical engine. Appl. Energy **122**, 247–260 (2014). https://doi.org/10.1016/j.apenergy.2014.01.071
17. Michler, T., Toedter, O., Koch, T.: Spatial and time resolved determination of the vibrational temperature in ignition sparks by variation of the dwell time. SN Appl. Sci (2020). https://doi.org/10.1007/s42452-020-3104-6
18. Dalziel, S.B., Hughes, G.O., Sutherland, B.R.: "Synthetic Schlieren [Konferenzbeitrag]." In: Proceedings of the 8th international symposium on flow visualization, 62.1–62.6 (1998)
19. Meier, G.E.A.: "Schlieren measuring process detects changes in turbulent atmospheric flow, aerodynamic, chemical processing and environmental pollution," DE19942856 (A1), DE DE19991042856 19990908, Jun 21, (2000)
20. Raffel, M.: Background-oriented schlieren (BOS) techniques. Exp. Fluids (2015). https://doi.org/10.1007/s00348-015-1927-5
21. Reimer, J., Bucherer, M., Pfeil, J., Koch, T.: "Analysis of the jet propagation of hydrogen and helium with PFI- and DI-injectors using BOS." In: Proceedings 12. Tagung Einspritzung und Kraftstoffe. Helmut Tschöke, Christian Reiser, Karsten Stenzel, pp 170–181 (2023)
22. Ben Hadj Ali, A.: Entwicklung eines CFD-Modells für Wasserabscheidung an einer gegengerichteten Wasser-Luft Schichtenströmung, (2014)
23. Seel, K., Reddemann, M.A., Baltaci, T., Kneer, R.: "Impact of Lubricating Oil Films on Spray-Wall Interaction." (2015) https://doi.org/10.4271/2015-01-2043
24. Seel, K., Reddemann, M.A., Kneer, R.: Optical investigation of the interaction of an automotive spray and thin films by utilization of a high-pressure spin coater. Exp. Fluids (2018). https://doi.org/10.1007/s00348-018-2505-4